Time-resolved interband transitions in periodic multilayer δ-doped systems

M. J. V. Bell
Universidade Estadual de Campinas, Caixa Postal 6165, CEP 13860-97, Campinas-SP, Brazil

D. F. de Sousa, V. Anjos, and L. A. O. Nunes
Instituto de Física de São Carlos, Universidade de São Paulo, Caixa Postal 369, CEP 13560-970, São Carlos-SP, Brazil
(Received 2 February 1998)

In this work we report a study of radiative interband recombinations in Si periodic multilayer GaAs systems. Photoluminescence and time-resolved photoluminescence measurements were performed, in order to discriminate band-to-band transitions, recombination of quantum confined electrons and photogenerated holes, as well as impurity assisted transitions. Results have been compared with self-consistent calculations, considering radiative recombination with heavy holes. [S0163-1829(98)02335-2]

I. INTRODUCTION

Since its first proposal, δ or planar doping has attracted considerable attention due to its unique electronic properties, extremely useful for the study of quantum confinement of carriers.[1–6] Furthermore, various potential technological applications on high speed electronic and photonic devices such as δ-FET, IR detectors, and tunable lasers have been reported.[7–9]

In particular, the relatively high silicon periodical planar doping of GaAs (typically $n_D > 10^{11}$ cm^{-2}) results in space-charge potential wells along the growth direction that confine the inhomogeneous electron distribution around the donor sheets.[1–6,10] For short period multilayer systems, strong coupling between adjacent wells gives rise to extended electronic densities that resemble uniformly doped systems. Therefore, the electronic states have a three-dimensional (3D) character. However, as the period is increased, the system tends to a set of isolated δ-doped wells. In this way, the electronic states are localized around each well exhibiting quasi-two-dimensional (2D) behavior. A very interesting situation occurs for intermediate periods, where Raman data show the coexistence of an admixture of 3D and 2D electrons.[10] As a result, two kinds of radiative interband emissions are possible. The first, called spatially indirect, is attributed to the recombination of 2D electrons, localized around the doping sheets, and photogenerated holes in the undoped region. The second, usually referred to as band to band or spatially direct, includes recombination of such holes and weakly localized electrons (3D).

Despite the great number of papers reporting on optical properties of δ-doped structures, to our knowledge, no clear characterization of indirect transitions has been presented.[1,4–6] Indeed, due to the small overlap between electron and hole wave functions, these transitions are intrinsically weak and experimental attempts for their detection have originated misinterpretation of spectra.[1,4] Surprisingly, transient measurements like time-resolved photoluminescence (TRPL) have not been explored so far, even though they could be extremely useful to discriminate direct and indirect transitions because the former are faster than the latter by about one order of magnitude. Nevertheless, few papers on TRPL have been reported on the literature.[2,3] In this respect, Dewdney *et al.*[2] have shown that for high periods and doping levels, sharp PL peaks (near the intrinsic fundamental gap of GaAs) appear, but only a part of the indirect transitions expected according to their calculations were identified. On the other hand, Henriques *et al.*[3] have dealt with only direct transitions.

In this work we report a detailed study of radiative interband recombinations in δ-doped superlattices, with periods of 20 and 50 nm and planar doping of 1.2×10^{12} and 1.0×10^{12} cm^{-2}, respectively, by using PL and TRPL. The former sample shows spatially direct radiative recombinations, with relaxation times about 200 ps. The latter presents a different picture. According to the calculated electronic structure, there are three sets of occupied subbands, E_0, E_1, and E_2 (henceforth called minibands), in which transitions to the valence band represented by E_0-hh, E_1-hh, and E_2-hh (where hh denotes heavy hole) are expected. The photoluminescence (PL) spectrum shows three structures, but only the spatially direct one (E_2-hh) is identified. The other ones are ascribed to acceptorlike transitions (C_{As}) and to phonon replica of E_2-hh. TRPL measurements revealed two additional peaks, not previously seen in the cw PL spectra, which were undoubtedly attributed to spatially indirect transitions corresponding to E_0-hh and E_1-hh. Their energy positions are in good agreement with the self-consistent calculations, and exhibit longer relaxation times about 1000 ps.

II. EXPERIMENTAL SETUP

The samples used in the present study consisted of thin sheets of silicon donors periodically implanted in single atomic monolayers during the molecular beam epitaxy (MBE) growth of an intrinsic GaAs film on a semi-insulating (001)-oriented GaAs substrate. The samples were grown at a temperature of 540 °C in order to reduce impurity diffusion.[11] The samples present interlayer spacings of 20 nm (sample 1) and 50 nm (sample 2) with planar densities of 1.2×10^{12} cm^{-2} and 1.0×10^{12} cm^{-2}, respectively, as measured by Hall effect. Both samples are 500 nm thick and are sandwiched between a 1-μm-thick buffer and cap layers cor-

responding to 20 nm and 50 nm for samples 1 and 2, respectively.

A standard PL setup was used in the PL experiments. The 514.5 nm line (2.41 eV) of an Ar^+ ion laser was used as an excitation source, operating in a low-excitation regime where the perturbation of the majority carrier population was negligible. The samples were cooled at 5 K, by He exchange gas in a continuous flow cryostat. The emitted light was dispersed in a 0.85-m double monochromator (SPEX 1403) and detected by a RCA 31034 GaAs photomultiplier, coupled to an electrometer (Keithley Instruments 610C).

TRPL was performed using the time-correlated single photon counting (TCSPC) technique.[12] The TCSPC system is composed of a Hamamatsu R380910-01 MicroChannel-Plate photomultiplier (MCP-PM), an EG&G ORTEC TC 455 TAC, a Tennelec 454 CFD discriminator, and an EG&G ORTEC SR553 timing single channel analyzer. The output of the analyzer was connected to a homemade photon counter interface. As an excitation source it was used a second harmonic line of a mode-locked Ti:sapphire laser (MIRA 900) tuned at 850 nm, providing a 425-nm wavelength (2.92 eV), repetition rate of 76 MHz and pulses of 250 fs. Also, an electro-optic modulator was used to reduce the repetition rate of the incident pulses, allowing an accurate determination of long recombination lifetimes as well as a better TAC performance.

III. RESULTS AND DISCUSSIONS

The self-consistent calculations of the electronic structure of samples 1 and 2 were performed at zero temperature with periodical boundary conditions using density-functional theory in the effective-mass approximation. It was assumed a Gaussian broadening distribution function for the donor sheet doping along the z axes with a full width at half maximum (FWHM) of 7 nm and a uniform distribution of negatively charged acceptors with density 1.0×10^{15} cm^{-3} for both samples.

In the low intensity photoluminescence regime, electron-hole pairs are generated with excess energy that relax through different nonradiative decay mechanisms. Under this condition there is a transient nonequilibrium phase in which the photoexcited electrons lose their excess energy and relax to the Fermi level of the conduction band and the photogenerated low-density hole rapidly thermalizes to the top of the valence subband (hh). These processes characterize the early ps lifetime of the carriers. During this short transient there are several interactions, such as intercarrier scattering and LO phonon interaction, which also depend on the carrier density and on the initial excess energy of the carriers. Optical transitions are achieved for recombination processes assuming momentum conservation. The PL line shape is determined by the product of the joint density of states (composed by the product of the density of states and the overlap of wave functions) and the thermal distribution of carriers, usually modeled by the Fermi-Dirac distribution and carrier temperature (depending on the photoluminescence excitation intensity), typically in the range from 10 to 60 K at a lattice temperature of 4 K. It was pointed out in Ref. 14 that while the joint density of states increases with energy, the thermal distribution decreases in such a way that PL line shape can present several sharp peaks.

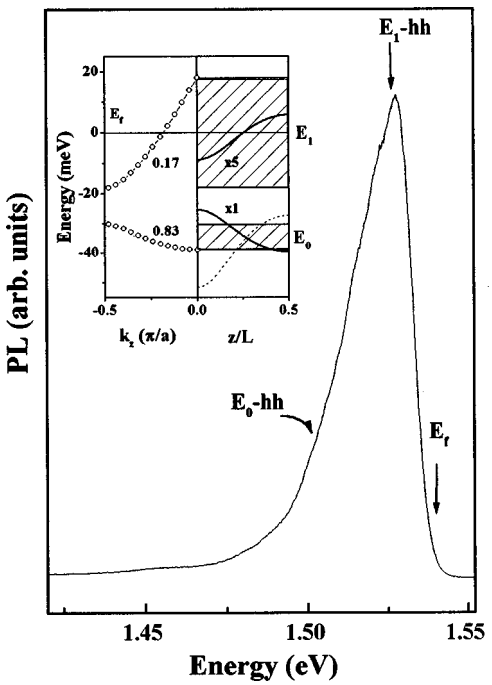

FIG. 1. Low-temperature (5 K) photoluminescence spectrum of a δ-doped superlattice (sample 1) excited at 2.41 eV. The vertical arrows mark the calculated interband transitions, according with the electronic structure illustrated in the inset. The calculations are for acceptor density of 1×10^{15} cm^{-3}, planar doping of 1.2×10^{12} cm^{-12}, and dopant spread of 7 nm. The heavy holes miniband is denoted by hh and E_F represents the Fermi energy.

Figure 1 shows photoluminescence from sample 1 as well as details of the conduction-band structure. The inset illustrates the zone center energy levels, where one can notice two minibands below the Fermi level (E_f), denoted by E_0 and E_1. Also shown are the potential profile (dashed line), occupation numbers, and relative probability densities (continuous lines) of each miniband. In this case, superlattice behavior takes place, as the interacting wells give rise to minibands with great dispersion. In order to calculate the interband transition energies, recombination with only heavy holes were taken into account. They are given by the difference between E_f (considered as a reference point) and the mean value of each miniband, as indicated by the arrows. In view of this, PL emission line shape is interpreted as the convolution of E_0-hh and E_1-hh transitions, with a low-energy threshold given by the bottom of the lowest conduction miniband E_0 and upper limit defined by the Fermi energy at 1.538 eV.

The PL spectrum of sample 2 is shown in Fig. 2(a). Electronic structure is shown in the inset. There are three minibands below the Fermi level, represented by E_0, E_1, and E_2. For the first one, electronic density is localized around the dopant spikes, similarly to isolated δ-doped samples. Nevertheless, E_1 and E_2 represent a quasicontinuum of nearly free electron states, reflected by the enhancement of miniband dispersion. Calculated interband transition energies, indicated by the arrows, clearly do not fit the bands observed in the spectrum. The more prominent band, at 1.515 eV, is associated to the convolution of E_1-hh and E_2-hh transitions. The enhanced wave-function overlap of electrons occupying E_2 and photogenerated holes explains the comparatively

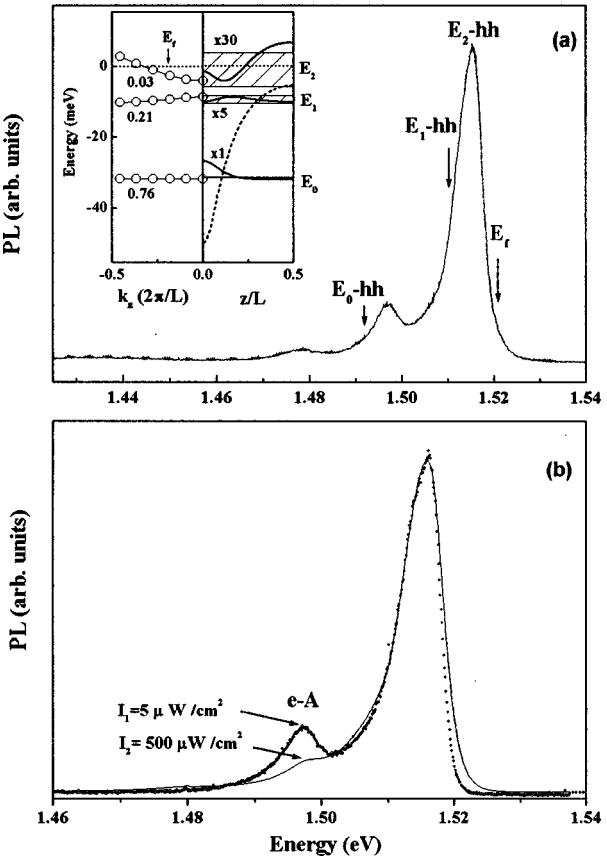

FIG. 2. Low-temperature (5 K) PL spectra of sample 2 excited at 2.41 eV. (a) The vertical arrows mark the calculated interband transitions, according to the electronic structure illustrated in the inset. The heavy hole miniband is denoted by hh and E_F represents the Fermi energy. (b) PL spectra as a function of excitation intensity. For low intensity ($I_1=5\ \mu$W/cm^2) e-A transition is clearly seen. With increasing excitation intensity ($I_2=500\ \mu$W/cm^2) saturation of acceptor impurities is achieved.

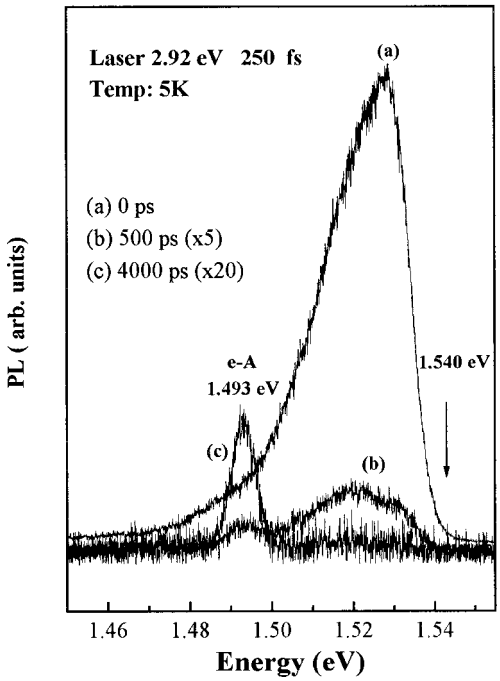

FIG. 3. TRPL spectra from sample 1, performed at 5 K with time delays of (a) 0 ps, (b) 400 ps, (c) 2000 ps, and (d) 4000 ps. Excitation energy is 2.92 eV.

strong emission intensity of this structure even though relatively few electrons occupy this miniband. The energy difference between the peak at 1.479 eV and the one at 1.515 eV corresponds exactly to one LO phonon. In this way, the former is ascribed to phonon replica of E_2-hh. On the other hand, the structure centered at 1.497 eV is attributed to free to bound transitions (e-A), also called band to acceptor transitions, and involves electrons from the E_2 and holes bound to acceptor impurities, unintentionally incorporated during MBE growth. Based on GaAs data, this peak is related to the carbon residual acceptor.[13,15] Additional support for our interpretation has been obtained by comparing PL spectra as a function of excitation intensity. Unintentional impurities are found in the samples with densities ranging from 10^{14} to 10^{15} cm^{-3}. Consequently, impurity assisted transitions show an intensity saturation behavior when excitation intensity is high enough to ionize all acceptor sites. This can be seen in Fig. 2(b), which displays the band to acceptor recombination as a function of intensity. At low excitation levels ($I=5\ \mu$W/cm^2), the e-A transition is more prominent, while as the intensity is increased to 500 μW/cm^2, the valence band is filled with photogenerated holes and the relative contribution from e-A decreases. When compared with intrinsic GaAs, the e-A transition shows an upshift of 3.5 meV, which corresponds to the difference between the mean position of the E_2 miniband and the top of the conduction-band potential profile. It is worth noting the small intensity of the e-A structure compared to the band-to-band transitions, indicating the small carbon content in the sample.

It should be noted that our conclusion differs from previous proposals,[1,4] which attributed the PL structures depicted in Fig. 2(a) to radiative recombination of the quantum confined electrons with the photogenerated holes.

Figure 3 shows the PL spectra at 5 K for sample 1 at different time delays after the laser excitation at 2.92 eV. The first one (curve *a*) is the time integrated PL spectrum, whose overall shape resembles very much that of the cw spectrum. As depicted in curve *b*, transitions E_0-hh and E_1-hh decay with almost equal recombination times about 200 ps, which are in good agreement with previously reported results in similar samples.[3] For longer delay times, as shown in curve *c*, only the e-A transition persists. Recombination time for this transition has been estimated to be 3500 ps.

In Fig. 4 are plotted the time-resolved PL spectra from sample 2, at 5 K under low excitation intensity. All curves are shifted in intensity for a better comparison. The spectra were recorded at different delay times of (a) 0 ps, (b) 200 ps, (c) 2000 ps, and (d) 5000 ps after the arrival of the excitation pulse. Just after excitation, the only difference with cw emission is the absence of the phonon replica band. With raising the time delay, two new structures, not previously seen in the cw spectrum, are detected. The first one is characterized by a shoulder on the low-energy side at 1509 eV for a delay time of 200 ps. In this curve, no emission from e-A transition is observed. The shoulder is better resolved in curve *c*, with a linewidth (FWHM) of about 10 meV. The second is a weaker band, which appears at 1.489 eV. Recombination times extracted from the PL decay are 290, 290, and 1200 ps,

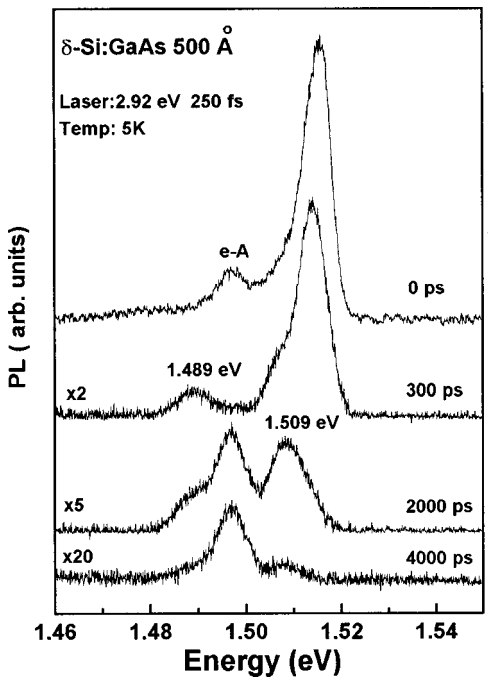

FIG. 4. TRPL spectra from sample 2 at 5 K with time delays of (a) 0 ps, (b) 500 ps, and (c) 4000 ps. Excitation energy is 2.92 eV.

for the emissions at 1.515, 1.509, and 1.489 eV, respectively, while the lifetime of the e-A transition is 3500 ps.

The bands at 1.489 and 1.509 eV are attributed to the spatially indirect radiative recombinations E_0-hh and E_1-hh, respectively. Further evidence for these assignments is provided by the calculated interband transitions, which are in reasonable agreement with the experiment, and also by the recombination times, longer than the spatially direct transition, as presented in Table I. Comparing results obtained for sample 2, it can be noted that theoretical values are shifted to higher energies, suggesting that real wells are deeper. One plausible explanation is that planar doping is higher than 1×10^{12} cm^{-2}. This is not surprising, since it was pointed out in Ref. 16 that Hall measurements underestimate the carrier density as well as the donor concentration by values up to 2. This effect is enhanced as the period increases, because more electrons are bounded near the dopant spikes and exhibit lower mobilities. Consequently, the Hall density represents only a mean value. According to our results, perfect agreement for all peak positions of sample 2 are obtained considering a planar doping of 1.2×10^{12} cm^{-2}. Similar results were obtained in resonant electronic Raman scattering performed on the same sample, which also exhibited a better agreement with experiment when 1.2×10^{12} cm^{-2} doping was considered.[10]

TABLE I. Results of TRPL for samples 1 and 2. It is presented a comparison between experimental (expt.) and theoretical (theor.) radiative transitions, as well as decay times.

Sample	Transition	Energy (expt.) eV	Energy (theor.) eV	Decay time (ps)
1	E_1-hh	1.530	1.528	200
	E_0-hh		1.519	200
	e-A	1.493	1.493	3500
2	E_2-hh	1.515	1.519	290
	E_1-hh	1.509	1.513	290
	E_0-hh	1.489	1.494	1000
	e-A	1.497	1.497	3500

The band at 1.489 eV could be attributed to a DAP (donor to acceptor pair) transition. This possibility is discarded by us because the recombination time for a DAP transition should be longer than the e-A one, as a consequence of the smaller overlap of wave functions between donors and acceptors, when compared to e-A. Moreover, it should also be present in cw PL and/or TRPL spectra of sample 1.

IV. CONCLUSIONS

We have presented a time-resolved radiative interband recombination study in δ-Si:GaAs superlattices, by PL and time-resolved PL techniques. It was shown that the short period superlattice resembles very much a 3D behavior, characterized by a broad PL emission band and short recombination time. On the other hand, the longest period superlattice presents an admixture of 3D and 2D electrons. In this case, PL emission exhibits spatially direct and indirect transitions, which were detected by TRPL. Further support for these assignments was yielded by the recombination times of the spatially indirect transitions, which were longer than those attributed to direct transitions. It should be noted that, to our knowledge, this is the first study that undoubtedly detects indirect transitions by spectroscopic techniques, which also exhibits a remarkable agreement with the self-consistent calculations.

ACKNOWLEDGMENTS

This work was supported by Conselho Nacional de Desenvolvimento Cientifico e Tecnologico (CNPq), Fundação de Amparo Pesquisa do Estado de São Paulo (FAPESP), and Coordenação de Aperfeiçoamento de Pessoal de Nível Superior (CAPES), Brazil.

[1] A. C. Maciel, M. Tatham, J. F. Ryan, J. M. Worlock, R. E. Nahory, J. P. Harison, L. T. Florez, Surf. Sci. **228**, 251 (1990).
[2] A. J. Dewdney, S. Holmes, H. Yu, M. Fahy, and R. Murray, Superlattices Microstruct. **14**, 205 (1993).
[3] A. B. Henriques, V. Bindilatti, N. F. Oliveira, Jr., and D. Heiman, Braz. J. Phys. **26**, 225 (1996).
[4] L. Chico, F. Garcia-Moliner, and V. R. Velasco, Phys. Rev. B **48**, 11 427 (1993).
[5] M. Ke, J. S. Rimmer, B. Hamilton, J. H. Evans, M. Missous, K. E. Singer, and P. Zalm, Phys. Rev. B **45**, 14 114 (1992).
[6] H. Maaref, H. Mejri, C. Priester, J. Barrau, G. Bacquet, and J. C. Bourgoin, J. Appl. Phys. **74**, 1987 (1993).
[7] K. Ploog, M. Hauser, and A. Fisher, Appl. Phys. A: Solids Surf. **45**, 233 (1988).
[8] F. Müller and F. Köch, Semicond. Sci. Technol. **6**, C133 (1990).
[9] E. F. Schubert, J. Vac. Sci. Technol. A **8**, 2960 (1990).

[10] V. Anjos, L. Ioriatti, and L. A. O. Nunes, Phys. Rev. B **49**, 7805 (1994).
[11] M. Santos, T. Sajoto, A. Zrener, and M. Shayegan, Appl. Phys. Lett. **53**, 2504 (1988).
[12] R. Cubeddu, F. Docchio, W. Q. Liu, R. Ramponi, and P. Taroni, Rev. Sci. Instrum. **59**, 2254 (1988).
[13] B. J. Skromme, G. E. Stillman, A. R. Calawa, and G. M. Metze, Appl. Phys. Lett. **44**, 240 (1984).
[14] *Delta Doping Semiconductors*, edited by E. F. Schubert (Cambridge University Press, Cambridge, 1996).
[15] *Properties of Gallium Arsenide* (INSPEC, London, 1986).
[16] R. C. Newman, M. J. Ashwin, M. R. Fahy, L. Hart, S. N. Holmes, C. Roberts, X. Zhang, and J. Wagner, Phys. Rev. B **54**, 8769 (1996).